Morphology and Thermal Stability of BR/Clay Composites Prepared by a New Method

Shaohui Wang, Yong Zhang, Zonglin Peng, Yinxi Zhang

Research Institute of Polymer Materials, Shanghai Jiao Tong University, Shanghai 200240, People's Republic of China

Received 9 March 2005; accepted 5 April 2005
DOI 10.1002/app.22153
Published online in Wiley InterScience (www.interscience.wiley.com).

ABSTRACT: A new potential preparation method named *in situ* organic modification was used to prepare intercalated polybutadiene rubber (BR)/clay/dimethyl dihydrogenated tallow ammonium chloride (DDAC) composites. That is, BR, pristine clay, and intercalatant DDAC were directly mixed in a Haake rheometer without pretreating the pristine clay with the intercalatant. The morphology of the BR/clay composites was investigated by means of X-ray diffraction and scanning electron microscopy. The thermal stability of the BR/clay composites was analyzed by thermogravimetric analysis (TGA). The dispersion of clay particles in the BR/clay/DDAC composites is much better than that in the BR/pristine clay and similar to that in the BR/organoclay DK4 (modified with DDAC) composites. BR/clay/DDAC composites have much higher thermal stability than the gum BR, BR/pristine clay, and BR/DK4 composites. The clay/intercalatant ratio has little influence on the thermal stability of the BR/clay/DDAC composites, while clay content has a significant effect on their thermal stability. The enhanced thermal stability of the BR/clay/DDAC composites is related to the dispersion state of clay particles in BR. © 2005 Wiley Periodicals, Inc. J Appl Polym Sci 99: 905–913, 2006

Key words: polybutadiene; rubber; clay; morphology; thermal properties

INTRODUCTION

Montmorillonite clay is a kind of special filler, with a layered structure. It has attracted much attention because of its capability in preparing polymer/layered silicate nanocomposites. One merit of such nanocomposites is the increased thermal stability.[1–4] The effect of clay on the thermal stability of thermoplastic matrices has been extensively investigated.[2,3,5] Blumstein[6] considered that the enhanced thermal stability of poly(methyl methacrylate) (PMMA)-based nanocomposites was not only due to differences in chemical structure (a decrease in the relative amount of PMMA endcapped by carbon–carbon double bond, as a result of reduced propensity to disproportionation reaction), but also due to restricted thermal motion of the macromolecules in the silicate interlayer. In explaining the obvious increase in the thermal stability of poly(dimethylsiloxane) nanocomposites, Burnside and Giannelis[1] attributed the increased thermal stability to hindered out-diffusion of the volatile decomposition products. However, Wang et al.[7] proposed other possible origins for the observed thermal stability improvement. That is, the active centers of silicone main chains' decomposition became inactive because of the interaction with the filler, or the unbuttoned degradation of silicone rubber was prevented by the increased physical and chemical crosslinking points built up between polymer chains and filler particles. Generally, the incorporation of clay into the polymer matrix was found to enhance thermal stability by acting as a superior insulator and mass transport barrier to the volatile products generated during decomposition.[5] Lepoittevin[8] found that both intercalated and exfoliated nanocomposites show higher thermal stability when compared to the pure poly(ε-caprolactone) or to the corresponding microcomposites. In addition, Lee et al.[9] found that the intercalated poly(ether imide) (PEI) nanocomposite is more stable than the delaminated PEI nanocomposite.

The effect of clay on thermal stability of elastomer nanocomposites is seldom reported. In our previous investigation,[10] a new potential preparation method named in situ organic modification was used to prepare polybutadiene rubber (BR)/clay composites, with good mechanical properties. That is, BR, pristine clay, and intercalatant (dimethyl dihydrogenated tallow ammonium chloride (DDAC)) were directly mixed in a Haake rheometer at a given temperature without pretreating the pristine clay with the intercalatants as usual. Alexandre et al.[11] used a similar method to prepare EVA/clay nanocomposite. They found that the thermal decomposition temperature during the second weight loss in air increased to about 35–40 K for all nanocomposites compared to the microcomposites. In this article, we prepared interca-

Correspondence to: Y. X. Zhang (yxzhang@sjtu.edu.cn).

Journal of Applied Polymer Science, Vol. 99, 905–913 (2006)

lated BR/clay composites by this method. The morphology of BR/clay composites was investigated by means of X-ray diffraction (XRD) and scanning electron microscopy (SEM). The thermal stability of BR/clay composites was analyzed by thermogravimetric analysis (TGA). The effects of clay/intercalatant ratio and clay content on the thermal stability of intercalated BR/clay composites were investigated.

EXPERIMENTAL

Materials

BR9000 was produced by Yanshan Petrochemical Co., Ltd., China. Pristine clay (Na-MMT, 80%) with a cation exchange capacity of 90 mequiv/100 g, organoclay DK4 (modified with about 40% DDAC), and intercalatant DDAC (75%) were provided by Zhejiang Fenghong Clay Chemicals Co., Ltd., China. All the other additives were industrial grade products.

Compounding and sample preparation

BR, pristine clay, and DDAC were melt mixed in a Haake rheometer RC90 (Haake Co., Germany) at 90°C at a rotor speed of 90 rpm for 6 min. Then, 2 phr stearic acid, 4 phr zinc oxide, 2.5 phr accelerator CZ (*N*-cyclohexylbenzothiazole-2-sulfenamide), and 1.5 phr sulfur were added to the aforementioned mixture at 30°C at 60 rpm and mixed for another 5 min. The resultant compounds were mixed further on a two-roll mill at ambient temperature for about 10 min. Finally, the compounds were compression-molded at 150°C under 10 MPa for an optimum cure time (t_{90}) to yield vulcanizates.

Measurement and characterization

Wide-angle XRD was used to study the expansion of the clay interlayer distance. The XRD patterns were obtained using a diffractometer (Dmax-rc, Japan) at the wavelength Cu Kα = 1.541 nm, with a generator voltage of 40 kV and a generator current of 100 mA. The diffractogram was scanned in the 2θ range from 1 to 20° at a rate of 4°/min. The interlayer distance of the clay layers, d, was calculated according to Bragg's equation.

The fracture morphologies of tensile samples were observed by SEM (Model *S*-2150, HITACHI) after the fractural surfaces were sputter-coated with gold.

TGA was carried out in a Perkin–Elmer TG analyser (Model TGA7) over a temperature range from room temperature to 800°C in a nitrogen flow at a heating rate of 20°C/min.

RESULTS AND DISCUSSION

XRD analysis

The XRD spectra for pristine clay, DDAC, and organoclay DK4 are shown in Figure 1. The pristine clay showed a single (001) diffraction peak at 2θ = 5.84°, corresponding to an interlayer distance of 1.51 nm. While the (001) diffraction peaks of DK4 obviously shifted toward low-angle direction, indicating the effective expansion of interlayer distance of clay. That is, the interlayer distance of clay expanded to about 2 nm from the original 1.51 nm. This expansion of gallery height was attributed to the intercalation of intercalatant chains by cation exchange reaction. This intercalation of alkylammonium increased the hydrophobicity of the clay and the affinity of clay to the BR matrix. The main diffraction peaks of DDAC were located at about 2.82°, 8.06°, 16.06°, and 18.96°. It is important to demonstrate here that the very strong diffraction peak of DDAC at about 2.82° is in the vicinity of the (001) diffraction peak of DK4. Thus, the characterization of intercalation of BR molecules becomes difficult, because of the interference of DDAC. Fortunately, no diffraction peak could be observed in the XRD spectrum of BR/DDAC vulcanizate [Fig. 2(c)]. That is, the displacement of (001) diffraction peak toward low-angle direction in relation to pristine clay still indicates the intercalation of BR molecules into the interlayer of clay.

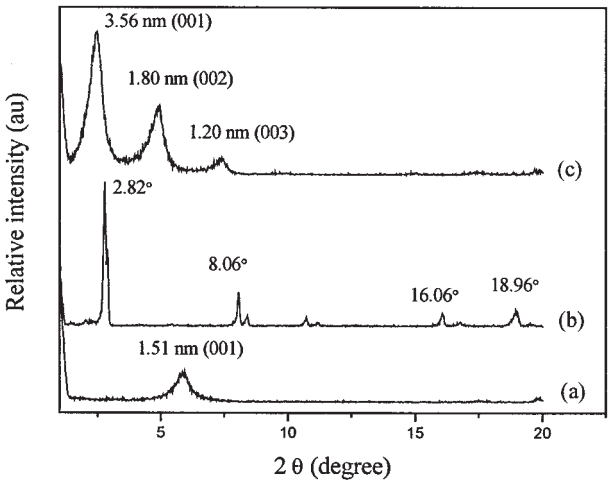

Figure 1 XRD spectra for (a) pristine clay, (b) DDAC, and (c) organoclay DK4.

As seen in Figure 2, the (001) diffraction peak of clay in the BR/pristine clay vulcanizate was located at 2θ = 6.02°, corresponding to an interlayer distance of 1.47 nm, which was just the same as pristine clay. This indicates that BR chains cannot intercalate into the gallery of pristine clay. The (001) diffraction peaks of clay in BR/DK4 and BR/clay/DDAC vulcanizates obviously shifted toward low-angle direction in relation to the corresponding organoclay DK4 and pristine clay, respectively. This means the expansion of the interlayer distance of clay. Moreover, the interlayer distance of BR/clay/DDAC vulcanizate is larger than that of BR/DK4 vulcanizate with the same composi-

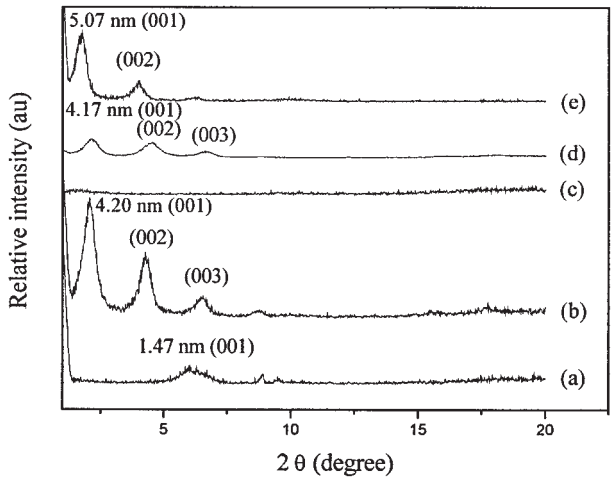

Figure 2 XRD spectra for (a) BR/pristine clay (100/18), (b) BR/DK4 (100/30), (c) BR/DDAC (100/12), (d) BR/clay/DDAC (100/18/12) compound, and (e) BR/clay/DDAC (100/18/12) vulcanizate.

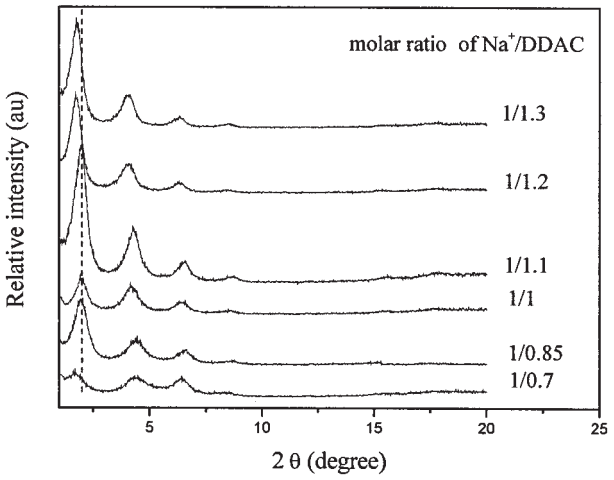

Figure 3 Effect of clay/DDAC ratio on XRD spectra of BR/clay/DDAC composite.

tion. The expansion of the interlayer distance is associated with the intercalation of BR molecules into the gallery of clay. So, intercalated BR/DK4 and BR/clay/DDAC composites were prepared. It is worth noticing that BR chains could intercalate into the gallery of pristine clay by simple melt mixing in the presence of DDAC. As seen in Figure 2(d), the interlayer distance of BR/clay/DDAC compound before vulcanization was 4.17 nm. This interlayer distance expanded to 5.07 nm [Fig. 2(e)] after the compound was vulcanized. The aforementioned facts indicate that intercalation occurred during mixing and this intercalation degree could be enhanced further by vulcanization. In the mixing stage, DDAC intercalated into the gallery of clay by cation exchange reaction even if no hot water acted as medium. That is, the clay was in situ organically modified. Obviously, the modified clay became organophilic. Its interlayer distance was expanded, and its surface energy was lowered. So, the modified clay is more compatible with BR, facilitating the intercalation of BR chains.

In addition, (002) and (003) diffraction peaks appeared in the XRD patterns of the BR/DK4 and BR/clay/DDAC vulcanizates. Joly et al.[12] observed the same phenomenon when they investigated dimethyl hydrogenated tallow (2-ethylhexyl) ammonium-modified montmorillonite/natural rubber nanocomposite. They explained that these harmonics were a strong indication of a very homogeneous swelling of the organo-modified montmorillonite, without exfoliation of the lamellae.

Figure 3 shows the effect of clay/DDAC ratio on XRD spectra of the BR/clay/DDAC composite. The clay/DDAC ratio is expressed by the molar ratio of Na^+ (which appears in the interlayer of clay) to DDAC, while the clay content is 20 phr. The (001) diffraction peak of clay slightly shifted to low-angle direction, with increasing DDAC content. The diffraction intensity of (001) diffraction peak increased with increasing DDAC content. This means that more intercalatants and BR molecules intercalated into the interlayer of clay, with increasing DDAC content.

In our previous investigation,[10] we found that the mechanical properties of BR/clay/DDAC composites were optimum when the molar ratio of Na^+ to DDAC equaled to 1/0.85. So, the Na^+/DDAC ratio of 1/0.85 was chosen to investigate the effect of clay content on XRD spectra of BR/clay/DDAC composite. The results are shown in Figure 4. Obviously, clay content has a little influence on the XRD spectra of BR/clay/DDAC composite.

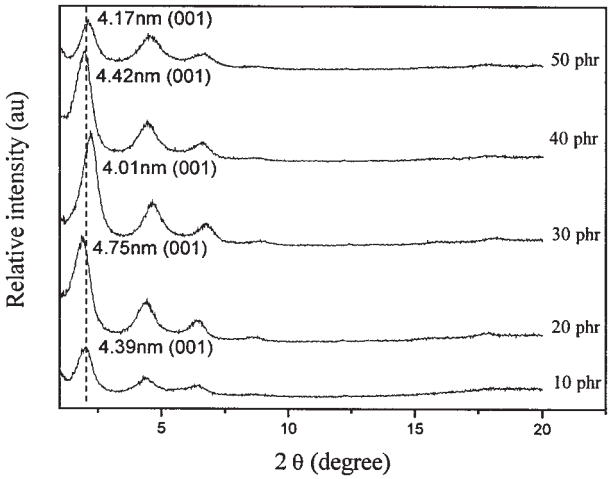

Figure 4 Effect of clay content on XRD spectra of BR/clay/DDAC composite.

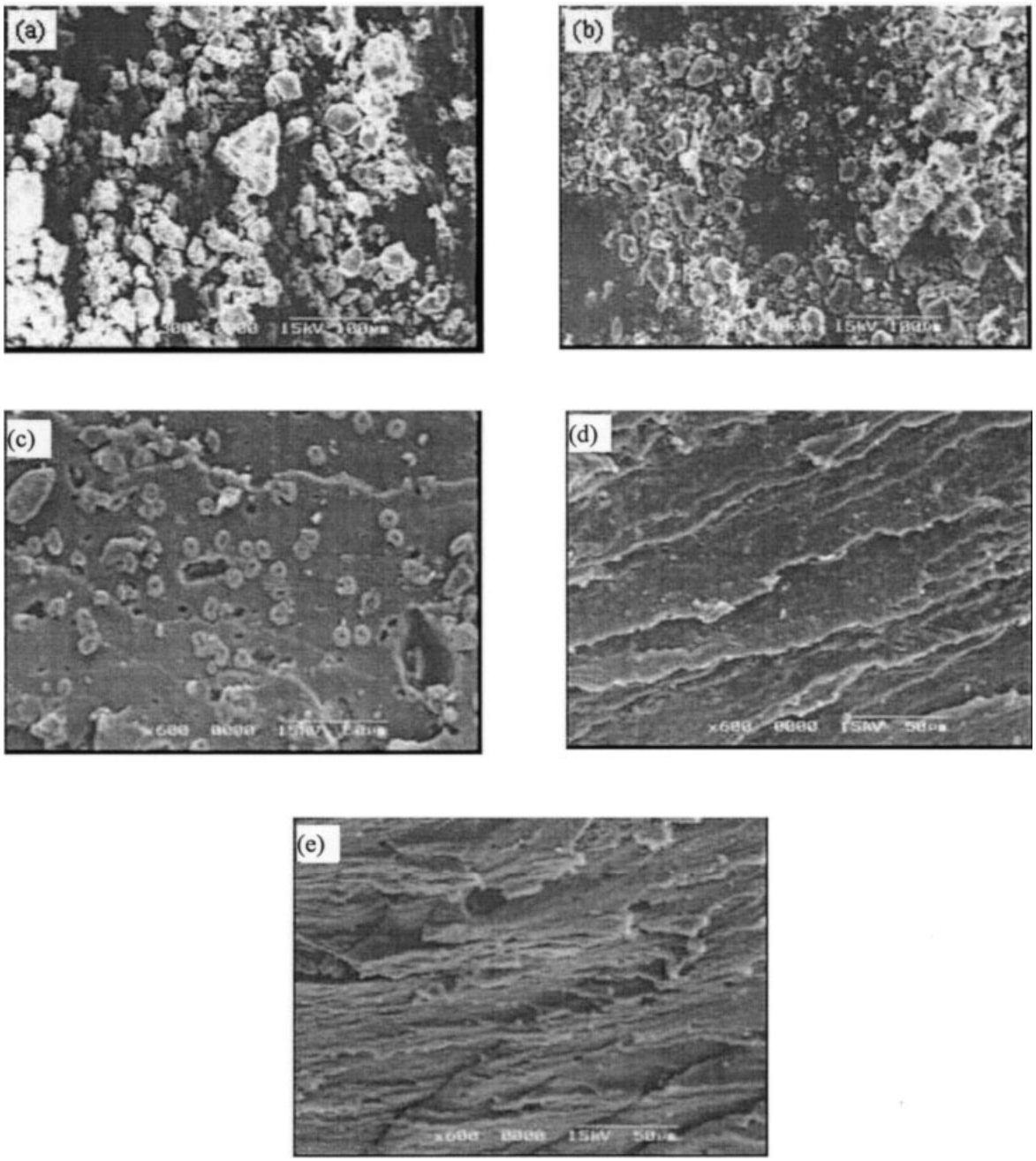

Figure 5 SEM photographs of (a) pristine clay and (b) organoclay DK4. Tensile fracture surface of (c) BR/clay (100/18), (d) BR/DK4 (100/30), and (e) BR/clay/DDAC (100/18/12) vulcanizates.

SEM observation

The tensile fracture morphologies of the BR/clay, BR/DK4, and BR/clay/DDAC vulcanizates are shown in Figure 5. To compare the sizes of clay particles before and after mixing with BR, the SEM photographs of pristine clay and organoclay DK4 are shown in Figures 5(a,b). The size of organoclay DK4 was a little smaller than that of pristine clay. Moreover, the distribution of DK4 particle size was more homogeneous than that of pristine clay.

There were a lot of large clay particles on the fracture surface of BR/clay vulcanizate [Fig. 5(c)]. The size of clay particles was smaller than that of pristine clay due to the shearing effect during the mixing process. The interface between the clay particles and the rubber matrix was distinct. Moreover, many microvoids that were attributed to the falling off of the clay particles from the rubber matrix under the stress were observed. These phenomena indicate that the compatibility and interaction between clay and rubber phase are poor.

The fracture morphologies of BR/DK4 and BR/clay/DDAC vulcanizates [Figs. 5(d,e)] were quite different from the BR/clay vulcanizate. Many parallel

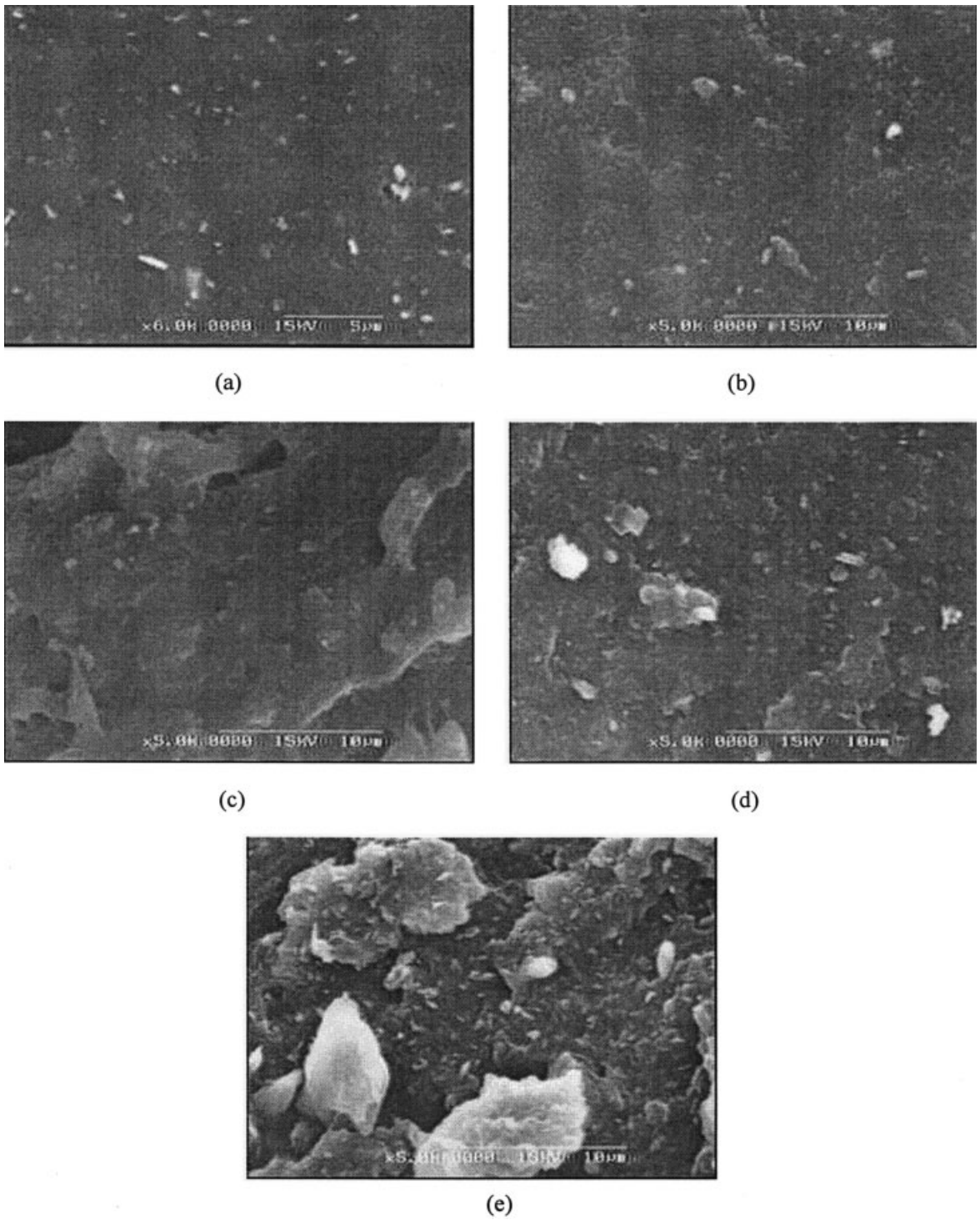

Figure 6 Effect of clay content on the morphology of BR/clay/DDAC composites observed by SEM: (a) 10 phr; (b) 20 phr; (c) 30 phr; (d) 40 phr; and (e) 50 phr.

strips were distributed on these fracture surfaces. In addition, the size of clay particles on the fracture surface of BR/DK4 and BR/clay/DDAC vulcanizates was much smaller than that in the BR/clay vulcanizate. Moreover, the interface between clay and BR was very blurry, indicating a stronger interface interaction.

Figure 6 shows the effect of clay content on the morphology of BR/clay/DDAC composites observed by SEM. No significant agglomeration of clay particles could be observed when the clay content was lower than 30 phr. The agglomeration trend of clay particles increased with increasing clay content. Large clay particles could be observed on the surface of composites when clay content exceeded 30 phr. This can be attrib-

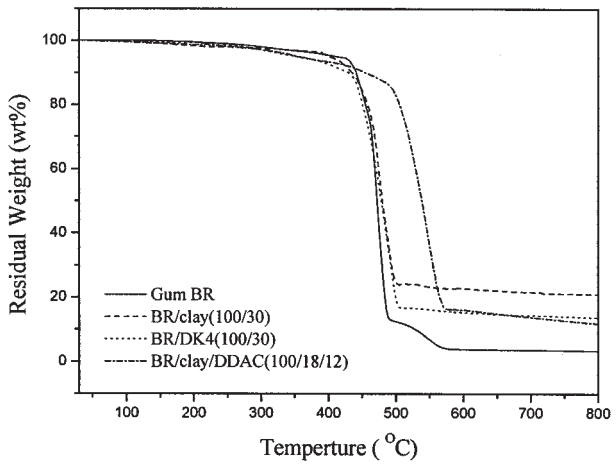

Figure 7 TGA thermograms of gum BR, BR/pristine clay, BR/DK4, and BR/clay/DDAC vulcanizates.

uted to the increase of contact opportunity of clay particles with increasing clay content.

TGA analysis

The thermal decomposition behavior of the gum BR, BR/pristine clay, BR/DK4, and BR/clay/DDAC vulcanizates was assessed by TGA. The results are shown in Figure 7. A slight increase in thermal decomposition temperature was observed for the BR/DK4 and BR/pristine clay vulcanizates in relation to the gum BR vulcanizate. However, the decomposition temperature greatly increased for the BR/clay/DDAC vulcanizate. The derivative thermogravimetric (DTG) curves of the aforementioned vulcanizates are shown in Figure 8. The temperature at degradation peak increased to 5°C, when pristine clay was added to BR. For DK4 and clay/DDAC, the temperature increased between 16 and 77°C, respectively. Obviously, clay/DDAC was much more effective in improving the thermal decomposition temperature of BR, which could be explained by good dispersion of clay particles in rubber matrix. This could be proved by the morphology observation from SEM mentioned earlier. The good thermal stability of BR/clay/DDAC composite is attributed to hindered out-diffusion of the volatile decomposition products.[1] The dispersion of DK4 in the rubber matrix was very good, but the thermal decomposition temperature of this vulcanizate was only slightly improved in relation to gum BR vulcanizate. The change of crosslinking density may be the reason for this phenomenon. In general, the thermal stability of vulcanizate increases with increasing crosslinking density when the decomposition energy of the crosslink is high.[13] It was found that the vulcanization degree of BR composite greatly decreased when DK4 was added into BR, as shown in our previous research.[10,14] The maximum torque (MH) of gum BR, BR/clay/DDAC, and BR/DK4 compounds measured by oscillating disk rheometer is 20.6, 20.8, and 16.7 dN m, respectively. The minimum torque (ML) of these compounds is essentially the same.[10] In general, the change of torque (ΔM = MH − ML) is proportional to the crosslinking density. So, we can conclude that the crosslinking density of BR/DK4 vulcanizate is obviously smaller than that of gum BR and BR/clay/DDAC vulcanizates. The effect of crosslinking degree partially counteracts the effect of good dispersion of clay particles on the thermal decomposition behavior of BR.

In addition, an interesting phenomenon could be observed from Figure 7. That is, the initial decomposition temperature of the BR composites decreased when organoclay DK4 or clay/DDAC were added into BR. Park,[15] Becker,[16] and Tang[17] found the same phenomenon when investigating Epoxy/Clay and PP/clay nanocomposites, respectively. The probable reasons may be that in nanocomposites the intimate contact between the polymer molecules and the atoms of the inorganic crystalline layers is more extensive than that in a microcomposite, and at the same time, there is a catalytic role played by the layered silicates deriving from the Hoffman reaction of C16, which may accelerate the charring process at the beginning of the degradation.[18]

To evaluate the thermal stability in detail, nonisothermal thermal degradation kinetics was calculated. In general, the reaction rate of thermal decomposition can be expressed as follows:

$$\frac{d\alpha}{dt} = k(1-\alpha)^n \tag{1}$$

where α is the fraction of reactant decomposed at time t, n is the order of the reaction, and k is the rate constant given by the following expression,

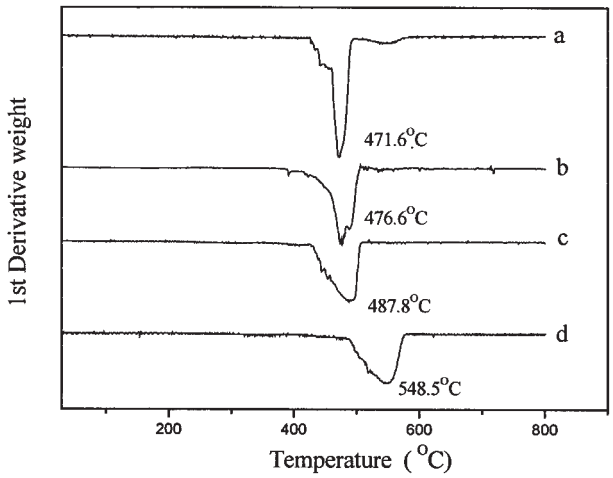

Figure 8 DTG curves of (a) gum BR vulcanizate, (b) BR/clay (100/30) vulcanizate, (c) BR/DK4 (100/30) vulcanizate, and (d) BR/clay/DDAC (100/18/12) vulcanizate.

TABLE I
Commonly Used g(α) forms for Solid State Reactions

Eq. No.	Form of $g(\alpha)$	Rate controlling process
1	$-\ln(1-\alpha)$	Random nucleation-one nucleus on each particle-Mampell equation
2	$1-(1-\alpha)^{1/2}$	Phase boundary reaction, cylindrical symmetry
3	$1-(1-\alpha)^{1/3}$	Phase boundary reaction, spherical symmetry
4	$\alpha+(1-\alpha)\ln(1-\alpha)$	Two dimensional diffusion
5	$(1-2/3\alpha)-(1-\alpha)^{2/3}$	Three dimensional diffusion sphere symmetry-Ginsthing-Brounshtein equation
6	$[-\ln(1-\alpha)^{1/2}$	Random nucleation-Avrami equation I
7	$[-\ln(1-\alpha)^{1/3}$	Random nucleation-Avrami equation II
8	$[1-(1-\alpha)^{1/3}]^2$	Three dimensional diffusion, sphere symmetry-Jander equation
9	α^2	One dimensional diffusion

$$k = A\, e^{-E/RT} \tag{2}$$

where A is the frequency factor and E is the activation energy of the reaction. For a linear heating rate of ϕ deg/min,

$$\phi = dT/dt \tag{3}$$

Thus, the reaction rate can be written as follows:

$$\frac{d\alpha}{dT} = \frac{A}{\phi}\, e^{-E/RT}(1-\alpha)^n \tag{4}$$

The overall decomposition rates are controlled by three fundamental aspects, namely, the laws of diffusion, nucleus formation and growth, and phase boundary movements. The most prominent rate controlling process operating in a particular case is chosen and used for deriving the rate equation. That is, different kinetic expressions could be obtained by integrating the earlier equation with different approximation treatments. Among those kinetic equations, Coats–Redfern equation is one of the well-known models:[19]

$$\lg\left[\frac{g(\alpha)}{T^2}\right] = \lg\left[\left(\frac{AR}{\phi E}\right)\left(1-\frac{2RT}{E}\right)\right] - \frac{E}{2.303RT} \tag{5}$$

A straight line will be obtained for the plot $\lg[g(\alpha)/T^2]$ versus $1/T$. The slope and intercept of this straight line can be used for calculating the kinetic parameters by the least squares method. The goodness of fit was tested by evaluating the correlation coefficient.[20] Nine equations, based on nine possible mechanisms [nine different forms of $g(\alpha)$], were chosen to describe the thermal decomposition reaction.[20] The form of $g(\alpha)$ that best represents the experimental data gives the proper mechanism. The nine possible equations and the rate controlling processes in each case are given in Table I. It was found that the rate controlling process of the gum BR, BR/pristine clay, and BR/DK4 composites followed random nucleation—Avrami equation II, while BR/clay/DDAC composite accorded with random nucleation—one nucleus on each particle—Mampell equation. The activation energy of degradation calculated by Coats–Redfern equation is 135, 142, 147, and 169 kJ/mol for the gum BR, BR/pristine clay, BR/DK4, and BR/clay/DDAC composites, respectively.

Figure 9 shows the effect of Na^+/DDAC ratio on the thermal stability of BR/clay/DDAC composites. No obvious variation could be observed. This means that Na^+/DDAC ratio has little influence on the thermal stability of BR/clay/DDAC composites.

The effect of clay content on the thermal stability of BR/clay/DDAC composites is shown in Figure 10. The effect of clay content on initial decomposition temperature (T_i, corresponding to 5% weight loss) and maximum temperature of the DTG peak (T_{max}) of BR/clay/DDAC composites is shown in Figure 11. T_i

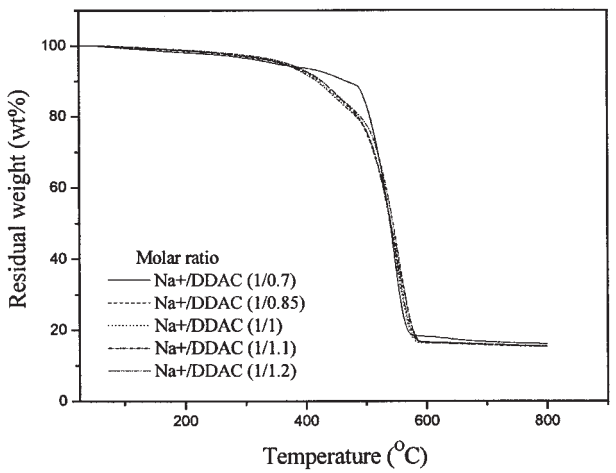

Figure 9 Effect of Na^+/DDAC ratio on TGA thermograms of BR/clay/DDAC vulcanizates.

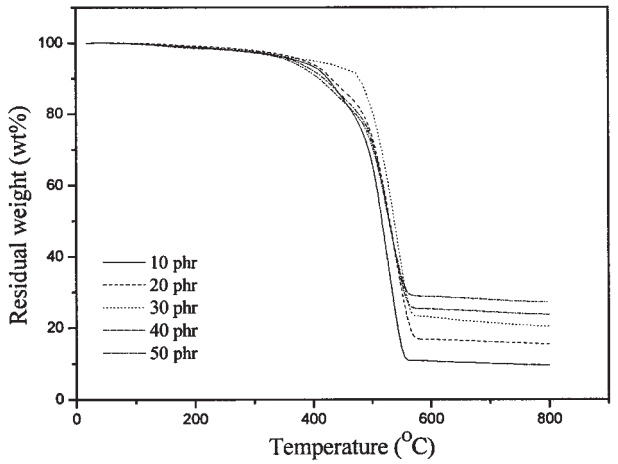

Figure 10 Effect of clay content on TGA thermograms of BR/clay/DDAC vulcanizates.

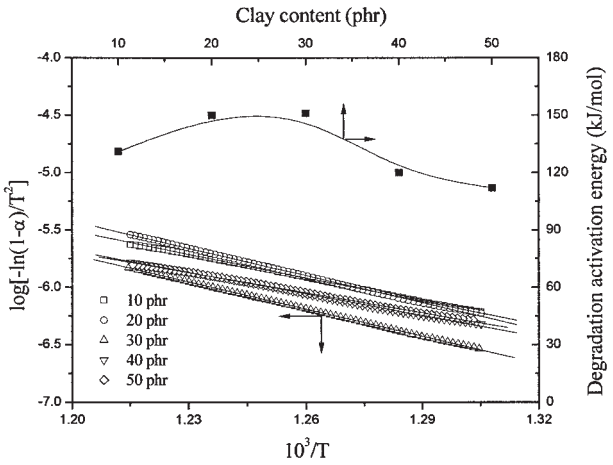

Figure 12 Effect of clay content on the activation energy of degradation.

and T_{max} reached their maxima at about 30 phr clay. The effect of clay content on degradation activation energy of BR was investigated by the Mampell equation. The results are showed in Figure 12. The degradation activation energy of BR increased with increasing clay content until the clay content reached 30 phr. Although clay content has little influence on the interlayer distance of clay in the BR/clay/DDAC composites, it has an important influence on the dispersion of clay particles in BR matrix as demonstrated in Figure 6. That is, obvious agglomeration of clay particles could be observed when the clay content exceeded 30 phr. The thermal stability of BR/clay/DDAC composites is associated with the dispersion state of clay particles in BR matrix. The clay layers with better dispersion state can act as superior heat insulators and physical barriers in mass transportation. Thus, the thermal stability enhances with increasing clay content. This effect will weaken when clay particles agglomerate.

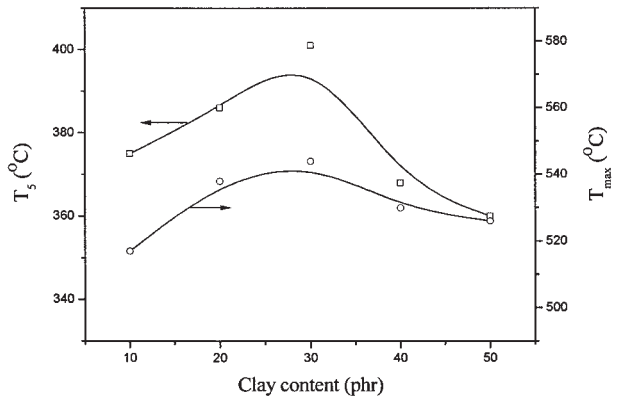

Figure 11 Effect of clay content on initial decomposition temperature (T_i) and maximum temperature of the DTG peak (T_{max}) of BR/clay/DDAC vulcanizates.

As aforementioned, the most important factors that influence the thermal stability of BR/clay composites are the dispersion state of clay particles.

CONCLUSIONS

Intercalated BR/clay/DDAC composites were prepared by a new method named *in situ* organic modification. The BR/clay/DDAC composites have much higher thermal stability than gum BR, BR/pristine clay, and BR/organoclay DK4 (modified with DDAC) composites. The clay/intercalatant ratio has little influence on the thermal stability of the BR/clay/DDAC composites, while clay content has a significant influence on their thermal stability. The dispersion of clay particles in the BR/clay/DDAC composites is much better than that in the BR/pristine clay composites and similar to that in the BR/DK4 composites. The clay particles in the intercalated BR/clay/DDAC composites aggregate with increasing clay content. The enhanced thermal stability of the intercalated BR/clay/DDAC composites is related to the dispersion state of clay particles in BR.

References

1. Burnside, S. D.; Giannelis, E. P. Chem Mater 1995, 7, 1597.
2. Alexandre, M.; Dubois, P. Mater Sci Eng R Rep 2000, 28, 1.
3. Gilman, J. W. Appl Clay Sci 1999, 15, 31.
4. Chang, Y. W.; Yang, Y.; Nah, C. Polym Mater Sci Eng 2001, 84, 591.
5. Ray, S. S.; Okamoto, M. Prog Polym Sci 2003, 28, 1539.
6. Blumstein, A. J Polym Sci Part A: Gen Pap 3 1965, 3, 2665.
7. Wang, S. J.; Long, C. F.; Wang, X. Y.; Li, Q.; Qi, Z. N. J Appl Polym Sci 1998, 69, 1557.
8. Lepoittevin, B.; Devalckenaere, M.; Pantoustier, N.; Alexandre, M.; Kubies, D.; Calberg, C.; Jerome, R.; Dubois, P. Polymer 2002, 43, 4017.
9. Lee, J.; Takekoshi, T.; Giannelis, E. Mater Res Soc Symp Proc 1997, 457, 513.

10. Wang, S. H.; Zhang, Y.; Peng, Z. L.; Zhang, Y. X. J Appl Polym Sci 2005, 98, 227.
11. Alexandre, M.; Beyer, G.; Henrist, C.; Cloots, R.; Rulmont, A.; Jérôme, R.; Dubois, P. Chem Mater 2001, 13, 3830.
12. Joly, S.; Garnaud, G.; Ollitrault, R. Chem Mater 2002, 14, 4202.
13. Yang, Q. Z. Modern Rubber Technology; China Petrochemical Press: Beijing, 1997; Ch. 2,4.
14. Wang, S. H.; Peng, Z. L.; Zhang, Y.; Zhang, Y. X. Polymers Polymer Compos 2005, 13, 371.
15. Park, S. J.; Seo, D. I.; Lee, J. R. J Colloid Interface Sci 2002, 251, 160.
16. Becker, O.; Varley, R. J.; Simon, G. P. Eur Polym J 2004, 40, 187.
17. Tang, Y.; Hu, Y.; Song, L.; Zong, R. W.; Gui, Z.; Chen, Z. Y.; Fan, W. C. Polym Degrad Stab 2003, 82, 127.
18. Zanetti, M.; Kashiwagi, T.; Falqui, L.; Camino, U. Chem Mater 2002, 14, 881.
19. Coats, A. W.; Redfern, J. P. Nature 1964, 201, 68.
20. Mathew, A. P.; Packirisamy, S.; Thomas, S. Polym Degrad Stab 2001, 72, 423.